

Coercivity Enhancement in $\text{Nd}_2\text{Fe}_{14}\text{B}$ Permanent Magnetic Powders through Rotating Diffusion Process with DyH_x Powders

Moonhee Choi¹, Jihun Yu², Donghwan Kim², Inbae Kim^{1*}, and Yangdo Kim^{1*}

¹Energy Materials Lab., School of Materials Science and Engineering, Pusan National University, Busan 609-735, Korea

²Functional Materials Powder Technology Group, Korea Institute of Material Science, Gyeongnam 641-831, Korea

(Received 5 September 2011, Received in final form 7 October 2011, Accepted 10 October 2011)

$\text{Nd}_2\text{Fe}_{14}\text{B}$ permanent magnetic powders ($iH_c = 9.2$ kOe, $B_r = 12.2$ kG) were produced by HDDR process. Their coercivity was enhanced to 12.6 kOe through the grain boundary diffusion process with dysprosium hydride (DyH_x). DyH_x diffusion process was optimized through rotating diffusion process, resulting in distinct phases rich in Nd and Dy observable by field emission scanning microscopy and transmission electron microscopy. The mechanism of coercivity enhancement that resulted in restrain the coupling effect between $\text{Nd}_2\text{Fe}_{14}\text{B}$ grains is also discussed.

Keywords : $\text{Nd}_2\text{Fe}_{14}\text{B}$, permanent magnet, diffusion process

1. Introduction

$\text{Nd}_2\text{Fe}_{14}\text{B}$ ternary rare earth magnets show higher maximum energy density product $(BH)_{\text{max}}$ and better intrinsic properties, such as saturation magnetization and magneto-crystalline anisotropy, than Sm-Co materials [1]. They have therefore been used in the motors of hybrid and electric vehicles. HDDR (Hydrogenation, Disproportionation, Desorption, and Recombination) can be used to form $\text{Nd}_2\text{Fe}_{14}\text{B}$ anisotropic magnetic powders [2], producing fine crystalline grains of avg. $0.3 \mu\text{m}$, close to single domain size [3, 4]. $\text{Nd}_2\text{Fe}_{14}\text{B}$ magnets require high coercivity for use in the high-performance motors of hybrid and electric vehicles and in other applications. The relatively low coercivity (avg. 10 kOe) of $\text{Nd}_2\text{Fe}_{14}\text{B}$ bond magnetic powders produced by HDDR greatly reduces their applicability. The substitution of Nd with rare earth elements such as Dy and Tb has been tested to improve the material's performance. The addition of Dy to $\text{Nd}_2\text{Fe}_{14}\text{B}$, resulting in $\text{Dy}_2\text{Fe}_{14}\text{B}$ created at the $\text{Nd}_2\text{Fe}_{14}\text{B}$ surface, can triple its magnetic properties. This is because the magnetization of Dy is higher than that of Nd and grain boundary phases in the Dy-diffused $\text{Nd}_2\text{Fe}_{14}\text{B}$ powders are thicker than in HDDR powders [5].

This work reports the optimization of Dy diffusion for

enhanced coercivity in $\text{Nd}_2\text{Fe}_{14}\text{B}$ powders, the mechanism of the enhancement is also discussed.

2. Experiment Procedure

Starting alloys of $\text{Nd}_{12.5}\text{Ga}_{0.3}\text{Nb}_{0.2}\text{B}_{6.4}\text{Fe}_{\text{bal}}$ were prepared by mold casting. $\text{Nd}_2\text{Fe}_{14}\text{B}$ magnetic powders were produced by HDDR of the mold-cast alloys. Dy diffusion precursors were prepared by ball-milling DyH_x powder under Ar for 5-20 hour. The powders were mixed at a ratio of $\text{DyH}_x:\text{Nd}_2\text{Fe}_{14}\text{B} = 3.4:96.6$, heated to $700\text{-}800^\circ\text{C}$,

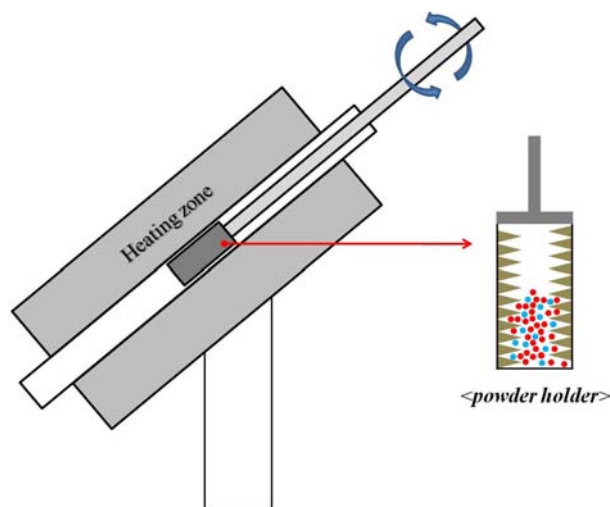


Fig. 1. (Color online) Furnace for rotating diffusion process.

*Corresponding author: Tel: +82-51-510-2478

Fax: +82-55-280-3289, e-mail: yangdo@pusan.ac.kr

and maintained at each temperature for 0.5-16 hours at 6×10^{-6} torr. The resulting Dy-diffused powders were then quenched to room temperature. And other experimental performed those mixed powders were heat-treated with continuous rotating at 1 rpm (Fig. 1). Magnetic properties were assessed using a VSM (Vibrating Sample Magnetometer, Lakeshore-7400) with a 14 T maximum field. Phase relations were analyzed by XRD (X-Ray Diffraction) with monochromated Cu $K\alpha$ radiation. Microstructure observation and compositional analysis were performed by FE-SEM (Field Emission Scanning Electron Microscopy), EDS (Energy Dispersive X-ray Spectroscopy), and TEM (Transmission Electron Microscopy).

3. Results and Discussions

$Nd_2Fe_{14}B$ magnetic powders were produced by HDDR [$iHc = 9.2$ kOe, $Br = 12.2$ kG], heated to 550-1,050 °C for 1 hr under vacuum, and then quenched to room temperature. The magnetic properties of the $Nd_2Fe_{14}B$ powders were studied at high temperature by VSM and XRD. Fig. 2 shows VSM results of the heated HDDR powders. Their coercivity and remanence greatly decreased with heating under vacuum, the lowest coercivity and remanence were observed at 1050 °C under vacuum.

Fig. 3 shows XRD patterns of the $Nd_2Fe_{14}B$ magnet powders at 850 °C under vacuum. Compared with HDDR powder, boron-rich (NdB_6), Nd-rich (Nd_2O_3), and soft magnet (α -Fe) phases were observed under vacuum heating. The powders' magnetic properties were greatly reduced ($iHc \leq 3$ kOe, $Br \leq 7$ kG, 850 °C) due to the secondary phases [6].

4.1 μm DyH_x powders have been reported to be most suitable for diffusion processing [7]. Powders' magnetic properties after various diffusion treatments with 4.1 μm

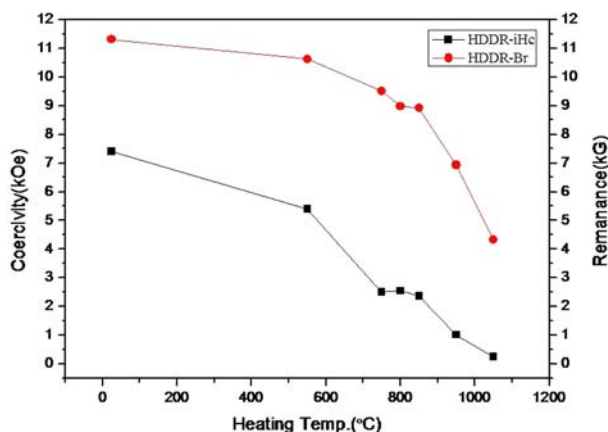


Fig. 2. (Color online) Magnetic properties of heated $Nd_2Fe_{14}B$ powders produced by HDDR under vacuum.

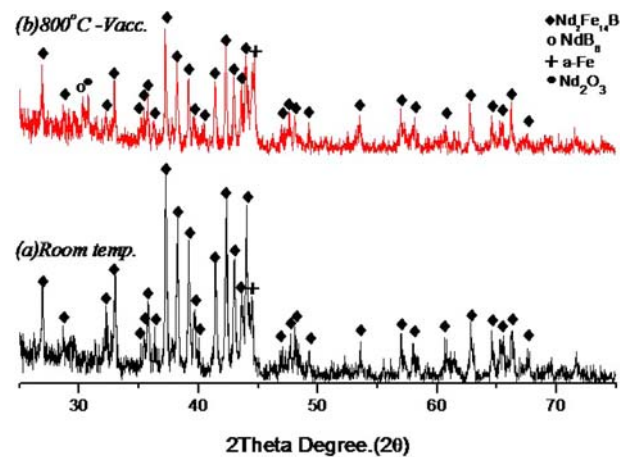


Fig. 3. (Color online) XRD patterns of heat-treated $Nd_2Fe_{14}B$ magnetic powders. (a) Original HDDR powders. (b) Powders after heating under vacuum.

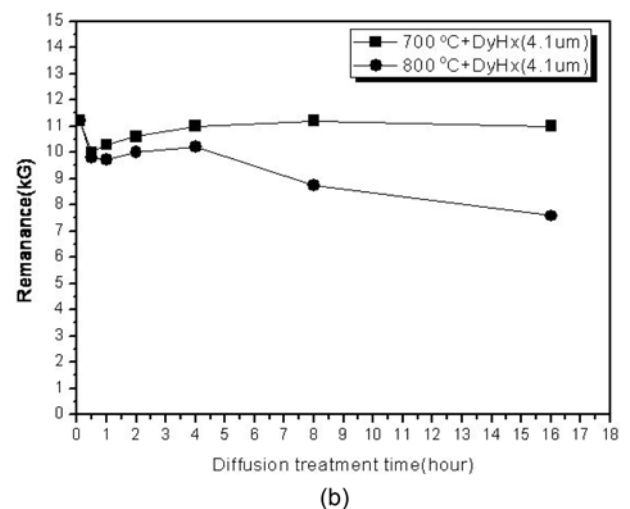
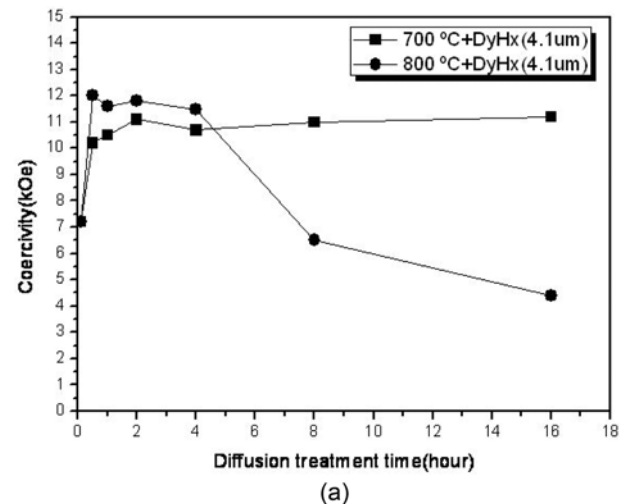


Fig. 4. (a) Coercivity and (b) remanence after diffusion treatment with 4.1 μm Dy at 700 and 800 °C for 0.5-16 hr at 6×10^{-6} torr.

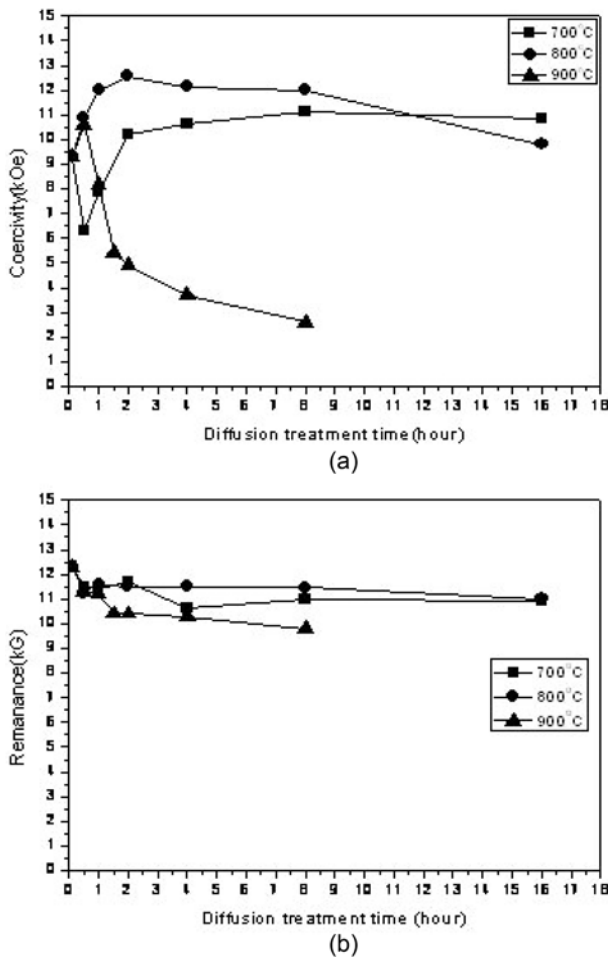


Fig. 5. (a) Coercivity and (b) remanence after rotating diffusion treatment with 4.1 μm Dy at 700, 800, and 900 $^{\circ}\text{C}$ for 0.5-16 hr at 6×10^{-6} torr.

Dy precursor are shown in Fig. 4. Coercivity increased to 12 kOe after diffusion treatment at 800 $^{\circ}\text{C}$ for 0.5 hr, from 9.2 kOe of the original Nd₂Fe₁₄B. Dy diffusion treatment for over 4 hr decreased coercivity by 7 kOe (Fig. 3(a)). Dy diffusion treatment decreased remanance by avg. 10% (Fig. 3(b)) because the volume fraction of Fe in the Nd₂Fe₁₄B phase decreased as Dy atoms substituted the Fe [8]. The antiparallel magnetic moment alignment of Dy and Nd₂Fe₁₄B also decreased remanance [9].

To improve diffusion efficacy and reduce AGG (Abnormal Grain Growth), diffusion treatment was tested under continuous rotation of the powder holder (at 1 rpm) that was inclined at 45 $^{\circ}$ (Fig. 4). The other conditions were as for NDP (Normal Diffusion Processing).

Fig. 5 shows powders' VSM results after RDP (Rotating Diffusion Processing) with 4.1 μm Dy precursor at 700-900 $^{\circ}\text{C}$ under high vacuum conditions. Coercivity increased to 12.6 kOe with RDP at 800 $^{\circ}\text{C}$ for 2 hr, but slightly

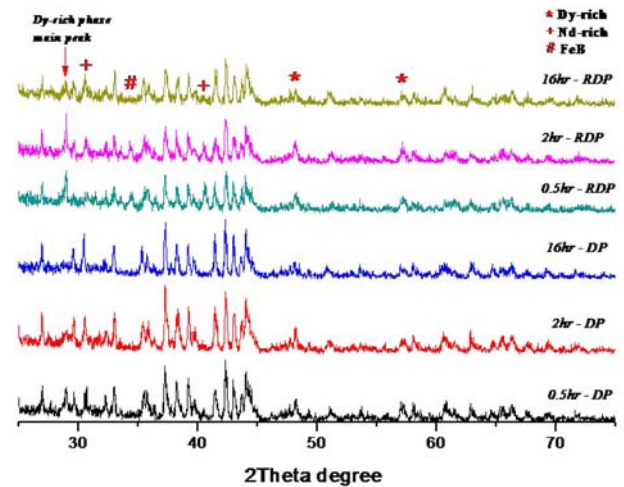


Fig. 6. (Color online) XRD patterns of Dy diffusion-treated Nd₂Fe₁₄B magnetic powders heated at 800 $^{\circ}\text{C}$ for 0.5-16 hr at 6×10^{-6} torr.

decreased with diffusion treatments of over 2 hr. The coercivity of powder after RDP at 900 $^{\circ}\text{C}$ decreased by 2.7 kOe.

Fig. 6 shows XRD patterns of powders after NDP and RDP at 800 $^{\circ}\text{C}$ for 0.5-16 hr under high vacuum. With normal processing, the Dy powder diffused at 800 $^{\circ}\text{C}$ within 0.5 hr, forming Dy and Nd-rich phases. Treatment over 2 hr decreased the XRD signals from the Dy-rich phases. RDP for 2 hr at 800 $^{\circ}\text{C}$ led to the formation of Dy-rich and Nd-rich phases; RDP for 16 hr resulted in weaker signals from the Dy-rich phases and increased signals from the Nd-rich phases.

Fig. 7 shows FE-SEM images of powders' surfaces after NDP and those of un-treated Nd₂Fe₁₄B powder. Powders that only underwent HDDR processing averaged 400 nm in size. NDP with 4.1 μm Dy precursor at 800 $^{\circ}\text{C}$ for 0.5 hr resulted in slightly larger particles (450 nm). Treatment for 16 hr resulted in much larger particles (850 nm). RDP produced smaller particles than NDP, giving average sizes of 430 and 682 nm after processing for 0.5 and 16 hr, respectively. EDS mapping analysis of powders after RDP for 0.5 hr showed that there was insufficient time for the Dy precursors to diffuse into the HDDR powders (Fig. 8). RDP for 2 hr resulted in slightly larger (435 nm) particles than RDP for 0.5 hr, verifying the diffusion of Dy precursors into the HDDR powders.

FE-SEM and EDS were used to study the effects of diffusion treatment duration on the magnetic properties of Nd₂Fe₁₄B powders after NDP. Dy was diffused at 800 $^{\circ}\text{C}$ for 0.5, 4 and, 16 hr. Fig. 9(a, b) shows cross-sectional BSE (BackScattered Electron) images of Nd₂Fe₁₄B powder after NDP for 0.5 hr. The surface region shows Dy atoms

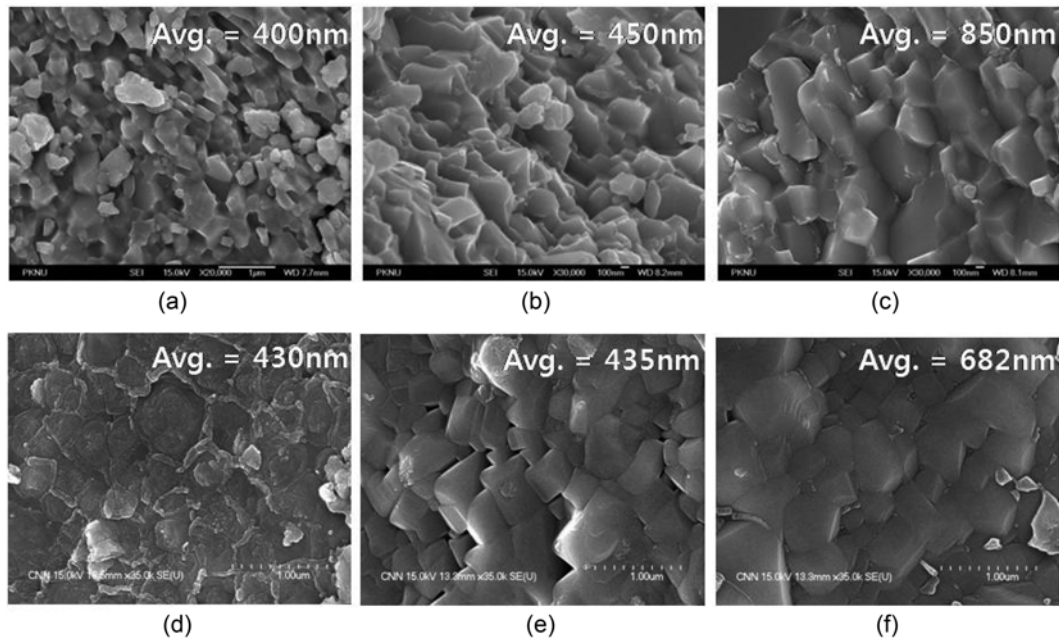


Fig. 7. FE-SEM images of $\text{Nd}_2\text{Fe}_{14}\text{B}$ powders' surfaces after normal and rotating Dy diffusion treatment at 800°C and 6×10^{-6} torr. (a) HDDR powders. Powders after normal diffusion processing for (b) 0.5 hr and (c) 16 h, and after rotating diffusion processing for (d) 0.5 hr, (e) 2 hr, and (f) 16 hr.

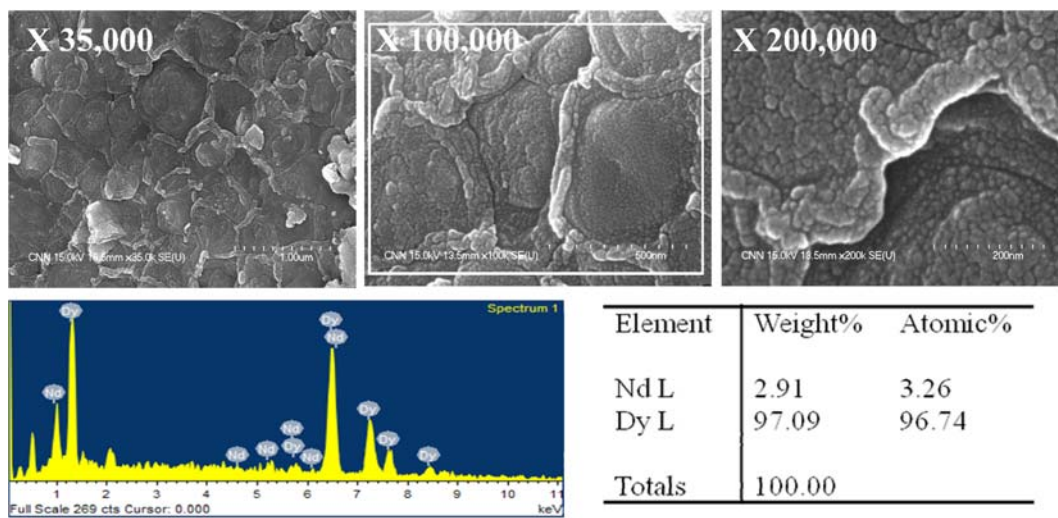


Fig. 8. (Color online) FE-SEM images of Dy diffusion-treated $\text{Nd}_2\text{Fe}_{14}\text{B}$ powders' surfaces after rotating process for 0.5 hr at 800°C and 6×10^{-6} torr.

present at 1.23-1.75 wt% (Fig. 10(a), Table 1). Phases rich in Nd and Dy were not observed close to the cores of the $\text{Nd}_2\text{Fe}_{14}\text{B}$ grains. The presence of grain boundary diffusion magnet phases, which interrupt coupling between $\text{Nd}_2\text{Fe}_{14}\text{B}$ grains, is confirmed in Fig. 9(b). Unlike after treatment for 0.5 hr, both coarse Nd and Dy-rich phases and vacancies were observed in the microstructure after 4 hr treatment (Fig. 9(c), Fig. 9(d)). Treatment for 16

hr resulted in AGG (Fig. 9(e)). Nd and Dy-rich phases and vacancies were observed because of the long treatment duration (Fig. 9(f)).

Cross-sectional BSE images were recorded for $\text{Nd}_2\text{Fe}_{14}\text{B}$ powders after RDP for 0.5 hr (Fig. 11(a)), 2 hr (Fig. 11(b), (c)), and 16 hr (Fig. 11(d)). The surface regions showed Dy precursor layers and fine Nd- and Dy-rich phases (Fig. 11(a)). Short diffusion treatment duration was shown

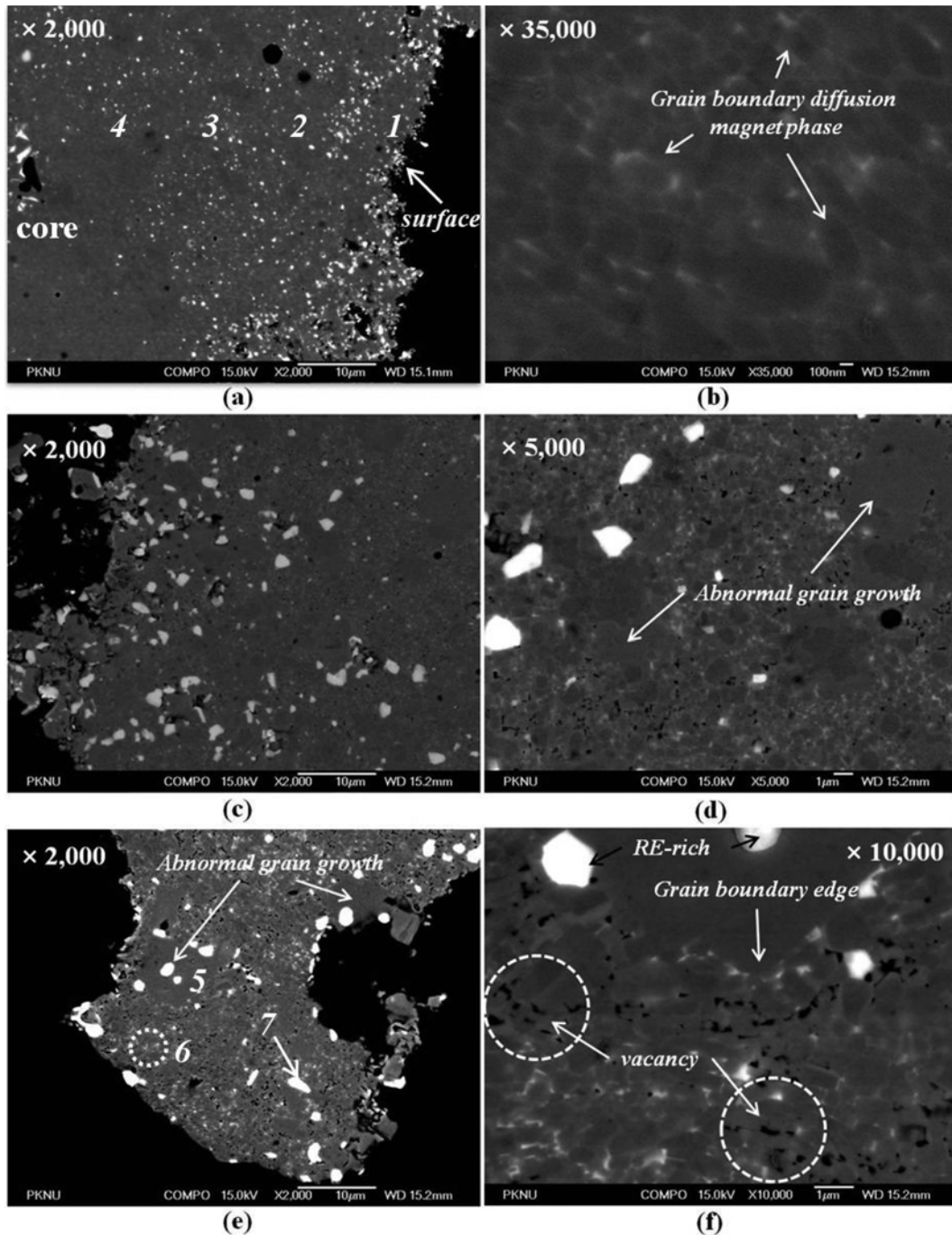


Fig. 9. Cross-sectional BSE images EDS analysis of Nd₂Fe₁₄B powders after non-rotating diffusion treatment at 800°C and 6 × 10⁻⁶ torr for (a, b) 0.5 hr, (c, d) 4 hr and (e, f) 16 hr.

to be unsuitable for RDP because Dy precursors were not thoroughly diffused into the HDDR powders. However, NDP was most suitable for 0.5 hr. For 2 hr diffusion treatment, it is observed that Dy precursors diffused into the HDDR powders and formation of grain boundary diffusion magnet phase. RDP for 16 hr resulted in Nd and Dy-rich phases and vacancies. However AGG, which was

observed after NDP for 16 hr, was not observed.

Fig. 12 shows TEM images after RDP at 800°C for 2 hr. Note that the single domain size of the initial HDDR Nd₂Fe₁₄B powder was avg. 400 nm, indicating that no appreciable grain growth occurred during RDP. EDS analysis showed rare-earth rich intergranular phases containing Nd and Dy. Grain boundaries were shown by EDS

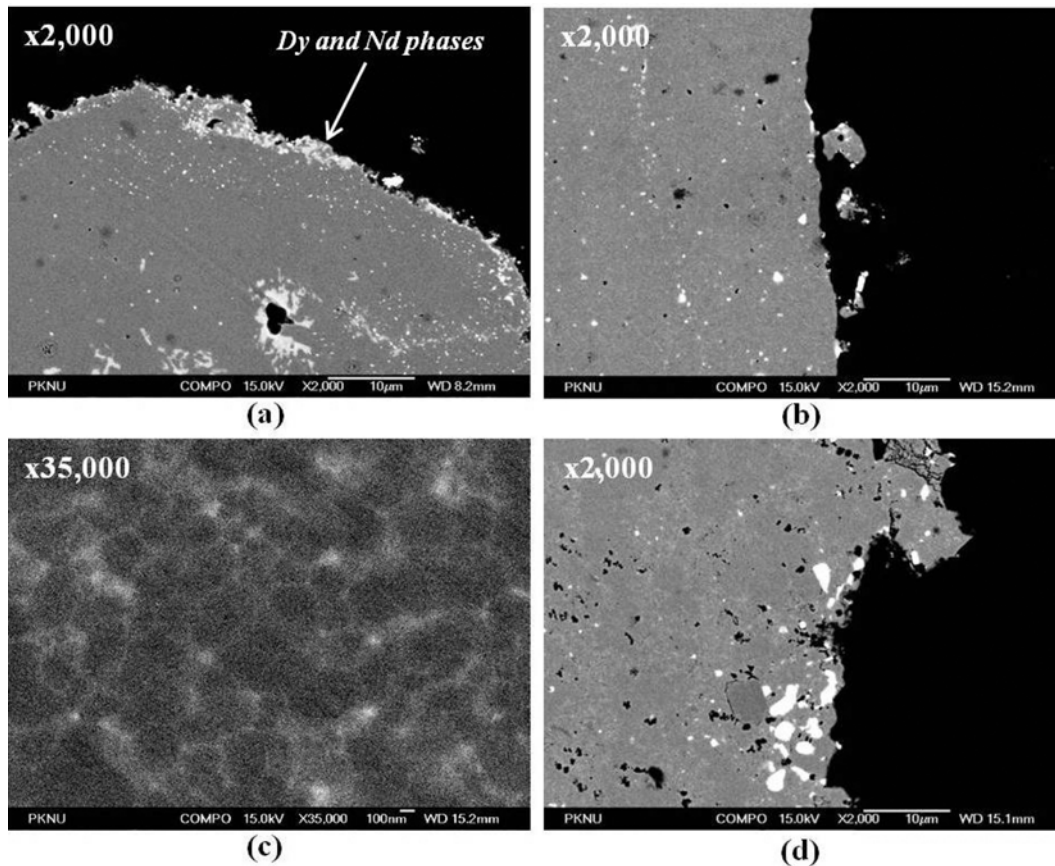


Fig. 10. Cross-sectional BSE images of $\text{Nd}_2\text{Fe}_{14}\text{B}$ powders after rotating diffusion treatment at 800°C and 6×10^{-6} torr for (a) 0.5 hr, (b, c) 2 hr and (d) 16 hr.

Table 1. EDS measurements after normal diffusion treatment at 800°C for 0.5 hr (1-4) and 16 hr (5-7).

	Nd (weight%)	Fe (weight%)	Dy (weight%)	Totals
1	28.15	70.10	1.75	100
2	29.09	69.45	1.46	100
3	28.82	69.95	1.23	100
4	25.79	74.21	–	100
5	24.96	72.23	2.72	100
6	35.56	65.38	0.76	100
7	85.20	5.49	9.32	100

mapping analysis to consist of Nd and Dy (Fig. 12(b), Table 2). Grain boundary thickness in HDDR $\text{Nd}_2\text{Fe}_{14}\text{B}$ has been reported to be 2 nm [10]. $\text{Nd}_2\text{Fe}_{14}\text{B}$ powders after RDP at 800°C for 2 hr at 10^{-6} torr showed 8 nm thick phases rich in Nd and Dy at the grain boundaries (Fig. 12(c)). The thicker grain boundaries containing Nd and Dy were effective in enhancing coercivity as they effectively interrupted coupling between the $\text{Nd}_2\text{Fe}_{14}\text{B}$ grains [11].

To increase coercivity in bond magnetic powders, it is

important to interrupt coupling and reduce AGG. AGG generally occurs with long heat treatment and decreases coercivity through the formation of grain boundary edges that create demagnetization fields (Fig. 9(f)) [12]. The formation of grain boundary diffusion phases was affected by the coercivity enhancement. The diffusion element, DyH_x , showed low solubility in the hard magnetic phases and formed additional intergranular rare earth-containing phases. These phases affected coupling between the $\text{Nd}_2\text{Fe}_{14}\text{B}$ grains. Nonmagnetic intergranular phases eliminated direct exchange interactions and also reduced long-range magnetostatic coupling between the $\text{Nd}_2\text{Fe}_{14}\text{B}$ grains. From the restraint the coupling effect, coercivity was increased (Fig. 9(b), 11(c), 13) [13].

Fig. 13 shows VSM results after various durations of NDP and RDP at 800°C . Coercivity was highest (12.6 kOe) after RDP for 2 hr, it slightly decreased with longer diffusion treatment. NDP was best for 0.5 hr, giving a coercivity of 12 kOe; 4 hr NDP decreased coercivity by 6 kOe. Coercivity was generally influenced by the particles' sizes. Longer NDP decreased coercivity because it induced abnormal grain growth and defects (vacancies, grain

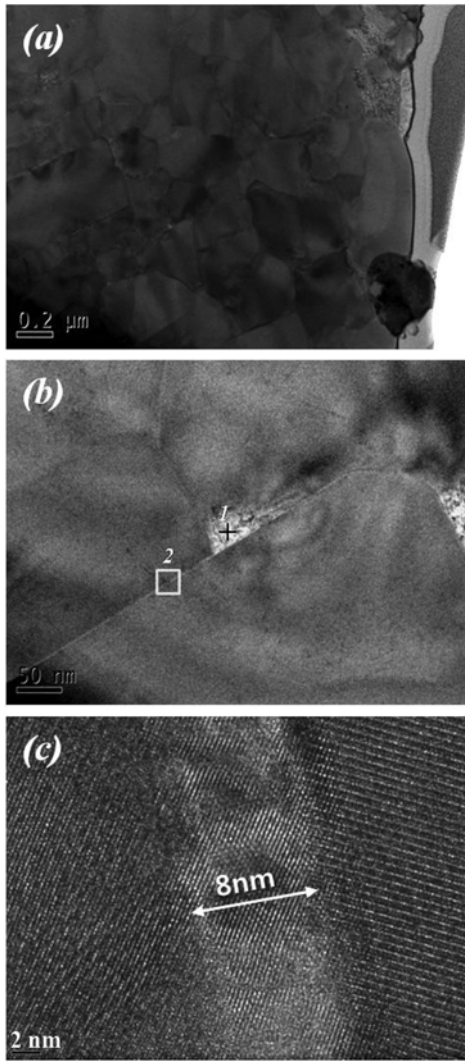


Fig. 11. High-resolution TEM images of Nd₂Fe₁₄B powders rotating diffusion treated at 800 °C for 2 hr at 6 × 10⁻⁶ torr.

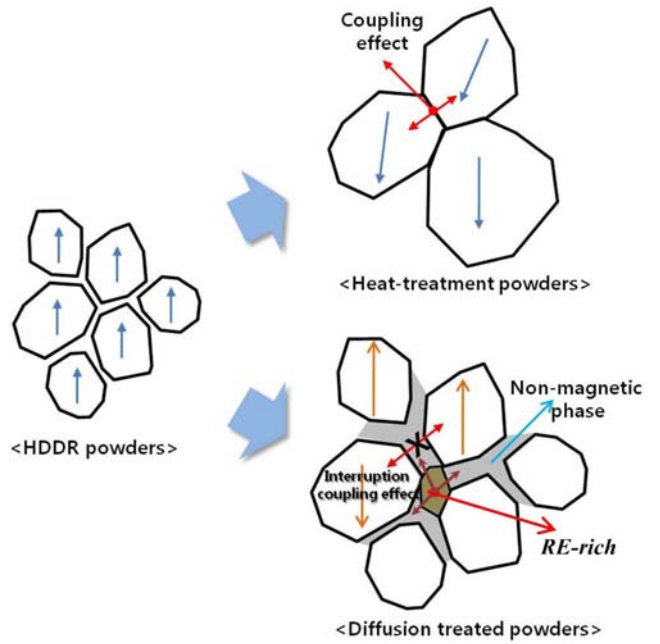


Fig. 12. (Color online) Nd₂Fe₁₄B grains in Dy diffusion-treated magnets.

Table 2. EDS measurements after rotating diffusion treatment at 800 °C for 2 hr.

Type	Memo	B	Fe	Nd	Dy	Total (Mass%)
EDS	1	0	7.7	88.3	3.9	100
EDS	2	0	88.4	10.6	1.0	100

boundary edges, surface cracks) (Figs. 7 and 9) [14]. RDP reduced grain growth and AGG in HDDR powders more than NDP (Figs. 7 and 11), leading to greater enhancements of coercivity than NDP.

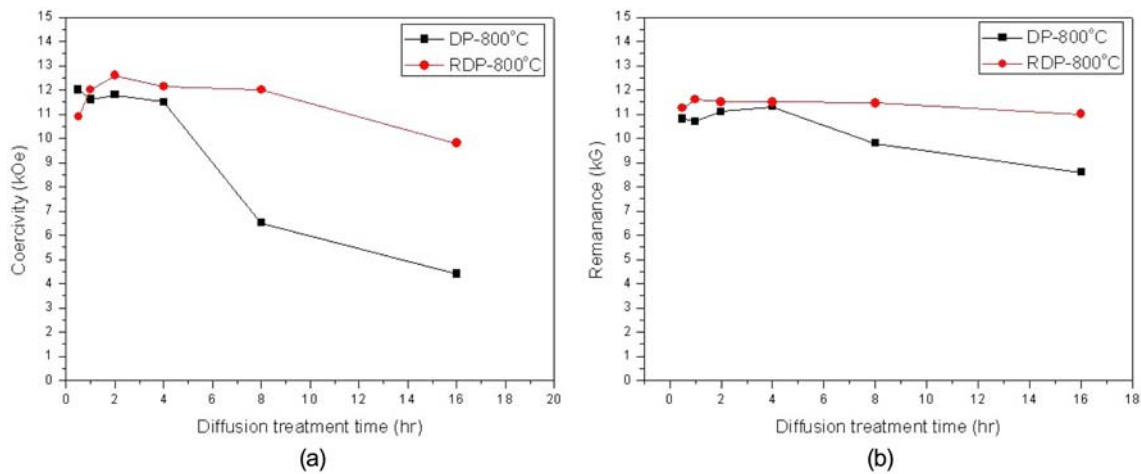


Fig. 13. (Color online) Magnetic properties of normal and rotating diffusion-treated Nd₂Fe₁₄B powders (a) coercivity, and (b) remanence.

4. Conclusions

The coercivity of Nd₂Fe₁₄B bond magnetic powders fabricated by HDDR was enhanced to 12.6 kOe by rotating diffusion processing with 4.1 μm DyH_x. Normal diffusion treatment enhanced coercivity best (*iHc* = 12 kOe) with short treatment for 0.5 hr at 800 °C. Rotating diffusion-treated powders showed highest coercivity (*iHc* = 12.6 kOe) after longer treated for 2 hr at 800 °C. Microstructure analysis of variously treated powders showed that the rotating diffusion led reduced AGG. Coercivity was higher after RDP than after NDP (Fig. 14), making RDP more suitable than NDP for enhancing coercivity in permanent bond magnetic powders. Coercivity enhancements were attributable to the increased thickness of the Nd- and Dy-rich grain boundary phases that interrupted coupling between the Nd₂Fe₁₄B grains.

Acknowledgements

The authors would like to acknowledge support from a grant from the Fundamental R&D program for Core Technology of Materials funded by the Ministry of Knowledge Economy, Republic of Korea.

References

- [1] Helmut Kronmüller and Stuart Parkin, Handbook of Magnetism and Advanced Magnetic Materials - Novel Materials, Wiley & Sons, West Sussex (2007) p.1946.
- [2] T. Takeshita and R. Nakayama, Workshop on Rare Earth Magnets and Their Applications, Pittsburg **1**, 49 (1990).
- [3] T. Takeshita and K. Morimoto, J. Appl. Phys. **79**, 5040 (1996).
- [4] J. Sujeung, Super Permanent Magnets, Ulsan University (2002) p.237.
- [5] J. Sujeung, Super Permanent Magnets, Ulsan University (2002) p.200.
- [6] Helmut Kronmüller and Stuart Parkin, Handbook of Magnetism and Advanced Magnetic Materials - Novel Materials, Wiley & Sons, West Sussex (2007) p.1958.
- [7] M. Choi, D. Kim, J. Yu, and Y. Kim, Rev. Adv. Mater. Sci. **28**, 34 (2011).
- [8] R. S. Mottram, B. Davis, V. A. Yartys, and I. R. Harris, Int. J. Hydrogen Energy **26**, 441 (2001).
- [9] Helmut Kronmüller and Stuart Parkin, Handbook of Magnetism and Advanced Magnetic Materials - Micro-magnetism, Wiley & Sons, West Sussex (2007) p.1027.
- [10] J. Sujeung, Super Permanent Magnets, Ulsan University (2002) p.353.
- [11] H. Sepehri-Amin, T. Ohkubo, and T. Nishiuchi, Scripta Materialia **63**, 1124 (2010).
- [12] Helmut Kronmüller and Stuart Parkin, Handbook of Magnetism and Advanced Magnetic Materials - Micro-magnetism, Wiley & Sons, West Sussex (2007) p.1028.
- [13] Helmut Kronmüller and Stuart Parkin, Handbook of Magnetism and Advanced Magnetic Materials - Micro-magnetism, Wiley & Sons, West Sussex (2007) p.1958.
- [14] B. D. Cullity, Magnetic Materials, ITC, Seoul (2003) p.542.